Classification of bladder cancer cell lines according to regulon activity

Aleyna ERAY[1,2] ⬤, **Serap ERKEK-ÖZHAN[1]** ⬤
[1]İzmir Biomedicine and Genome Center, İzmir, Turkey
[2]Dokuz Eylül University İzmir International Biomedicine and Genome Institute, İzmir, Turkey

Abstract: Bladder cancer is one of the most frequent cancers and causes more than 150.000 deaths each year. During the last decade, several studies provided important aspects about genomic characterization, consensus subgroup definition, and transcriptional regulation of bladder cancer. Still, much more research needs to be done to characterize molecular signatures of this cancer in depth. At this point, the use of bladder cancer cell lines is quite useful for the identification and test of new signatures. In this study, we classified the bladder cancer cell lines according to the activities of regulons implicated in the regulation of primary bladder tumors. Our regulon gene expression-based classification revealed three groups, neuronal-basal (NB), luminal-papillary (LP), and basal-squamous (BS). These regulon gene expression-based classifications showed a quite good concordance with the consensus subgroups assigned by the primary bladder cancer classifier. Importantly, we identified *FGFR1* regulon to be involved in the characterization of the NB group, where neuroendocrine signature genes were significantly upregulated, and further β-catenin was shown to have significantly higher nuclear localization. LP groups were mainly driven by the regulons *ERBB2*, *FOXA1*, *GATA3*, and *PPARG*, and they showed upregulation of the genes involved in epithelial differentiation and urogenital development, while the activity of *EGFR*, *FOXM1*, *STAT3*, and *HIF1A* was implicated for the regulation of BS group. Collectively, our results and classifications may serve as an important guide for the selection and use of bladder cancer cell lines for experimental strategies, which aim to manipulate regulons critical for bladder cancer development.

Key words: Bladder cancer, classification, regulon, gene regulation, neuroendocrine

1. Introduction

Bladder cancer is a heterogeneous group of tumors, where transitional cell carcinoma constitutes the great majority of the cases. Classically, bladder cancer is diagnosed in two histopathological classes as 'muscle invasive bladder cancer (MIBC)' and 'non-muscle invasive bladder cancer (NMIBC)' with different prognostic and molecular characteristics (Jin et al., 2014). In the last decade, there have been a number of studies characterizing the genomic landscape of both MIBC and NMIBC and defining the molecular subgroups (Cancer Genome Atlas Research 2014; Hedegaard et al., 2016; Robertson et al., 2017; Tan et al., 2019). A more recent study aimed to define the consensus subgroups of MIBC using the gene expression data in combination with several studies (Kamoun et al., 2020), where the six consensus subgroups were referred to as 'luminal papillary', 'luminal nonspecified', 'luminal unstable', 'stroma-rich', 'basal/squamous', and 'neuroendocrine-like'. In this study, the authors, in addition, associated these subgroups with distinct regulon activities, previously defined in (Robertson et al., 2017).

These regulons implicated in bladder carcinogenesis include transcription factors and growth factor receptors, determined according to their gene regulatory activity in bladder cancer (Robertson et al., 2017).

Bladder cancer cell lines have been extensively used for modeling the development, progression and molecular characteristics of bladder cancer. In addition to the focused characterization of cell lines, where only two/three of them are used (Piantino et al., 2010; Pinto-Leite et al., 2014), there are a few other studies, which provided details about the molecular and genomic characterization of bladder cancer cell lines collectively. In one study, a classification based on the subgroups defined by (Sjodahl et al., 2012), '"Urobasal A", "Urobasal B", "Genomically Unstable"and "SCC-like" were established for 40 bladder cancer cell lines (Earl et al., 2015). Another study performed exome sequencing for 25 bladder cancer cell lines and identified the frequently mutated genes among analyzed cell lines (Nickerson et al., 2017). A more recent study provided a comprehensive review about molecular characteristics, origin, and tumorigenic properties of more than 150

murine and human bladder cancer cell lines (Zuiverloon et al., 2018). In addition, the Cancer Cell Line Encyclopedia of the Broad Institute (CCLE database) provides a unique source for the transcriptomic and genomic data produced in a variety of cancer cell lines including bladder cancer (Barretina et al., 2012).

Although regulon activities have been significantly associated with primary bladder cancer subgroups (Robertson et al., 2017; Kamoun et al., 2020), there has not been yet a study, which characterized the bladder cancer cell lines according to regulon activities defined for the primary bladder cancers (Robertson et al., 2017; Kamoun et al., 2020). In this study, we classified the bladder cancer cell lines into 3 groups according to their regulon activities and associated the upregulated genes in each cell line group with the targets of the regulons. Our results reveal previously unknown cooperative regulatory activities in bladder cancer cells and can serve as a guide for modeling bladder cancer according to different regulon activities.

2. Methods

2.1. Experimental methods

2.1.1. Cell culture

The two bladder cancer cell lines 5637 and RT112 were obtained from DSMZ and J82 was kindly provided by Dr. S. Senturk (Izmir Biomedicine and Genome Center, Izmir). 5637 and RT112 were cultured in RPMI 1640 (Gibco BRL), J82 was cultured in DMEM (Dulbecco's Modified Eagle Medium). All media were supplemented with %10 FBS and %1 Penicillin-Streptomycin. Cells were cultured at 37 °C and 5% CO_2.

2.1.2. Immunofluorescence

In 24 well plates, J82 was plated 10000/well, RT112 was plated 20000/well, 5637 was plated 40000/well. Cells were incubated overnight on glass coverslips and rinsed with 1x PBS the following day. Cells were fixed with 4% formaldehyde for 15 min at RT, and 0.2% TritonX was used for permeabilization. Fixed cells were blocked with 2% Donkey serum for 45 min. Afterwards, cells were incubated with β-catenin antibody (1:100, #9562, Cell Signaling) diluted in 2% donkey serum overnight at 4°C. Next day, cells were rinsed 2 times with 1x PBS. Goat Anti-Rabbit Alexa Fluor 594 was used as a secondary antibody. DAPI was used for nucleus staining. Coverslips were mounted onto slides for imaging with Zeiss LSM880. Images were acquired as Z-stack using ZEN 2 software. Images with maximum intensity were used for further analysis. Quantification of the images were done with ImageJ program. Splitted DAPI channel images were used to determine region of interests for nuclear β-catenin signal intensities. A total of 17 cells per cell line were used for quantification. Integrated Density Values (IDV) were used for statistical analysis.

2.2. Data acquisition

CCLE RNAseq gene expression data for bladder cancer cell lines (RPKM) were downloaded from Cancer Cell Line Encyclopedia (CCLE) database (Barretina et al., 2012) and were accessed at cbioportal (Cerami et al., 2012; Gao et al., 2013). Regulon definitions were based on (Robertson et al., 2017; Kamoun et al., 2020). Mutation data for bladder cancer cell lines were obtained using cbioportal (Cerami et al., 2012; Gao et al., 2013). Neuroendocrine differentiation gene definitions are based on the information provided in Supplementary Table 3 from (Kamoun et al., 2020).

2.3. Data analysis

2.3.1. Clustering of the cell lines according to regulon expression levels

Using the gene expression values for the regulon genes, we clustered 25 bladder cancer cell lines using kmeans option (k = 6), within pheatmap package (Kolde 2019). Only the regulons that have min 1 rpkm (log2 scale) expression value in at least one cell type analyzed were included in clustering. This resulted in 19 number of regulons which contributed to the clustering analysis.

#### 2.3.2. Consensus classification of bladder cancer cell lines

In order to determine the consensus classification of bladder cancer cell lines, we utilized the "Molecular Classification of Bladder Cancer" classifier developed by Kamoun et al., (Kamoun et al., 2020) (134.157.229.105:3838/ BLCAclassify). Gene expression matrix for the cell lines in rpkm (obtained from CCLE database (Barretina et al., 2012)) was uploaded to the classifier and resulting consensus classifications are presented in Figure 1b and Supplementary Table S1.

2.3.3. Differential gene expression analysis

Differential gene expression analysis, where one cell line group was compared with the other groups, was performed using cbioportal (Cerami et al., 2012; Gao et al., 2013). Basically, custom cell line groups were formed based on our classifications (Figure 1), and differentially expressed genes were identified using 'Compare' and 'mRNA' options. Upregulated genes were defined using q value threshold of 0.1 and log Ratio of 0.5.

2.3.4. Gene ontology analysis and visualization

Gene ontology analysis for the upregulated gene sets was performed using the ConsensusPathDB (CPDB) database of Max Planck Institute (Kamburov et al., 2009; Kamburov et al., 2011). Overrepresentation function of the CPDB was used, and only Level 4 GO terms (Biological Process) were included for further analysis. "GOChord" function of "GOplot" R package was used for visualization (Walter et al., 2015). In chord graphs, maximum top 20 GO terms with adjusted p-value <0.05 were shown. For the limit parameter of the "GOChord" function, a minimum number of genes belonging to a specific GO term was
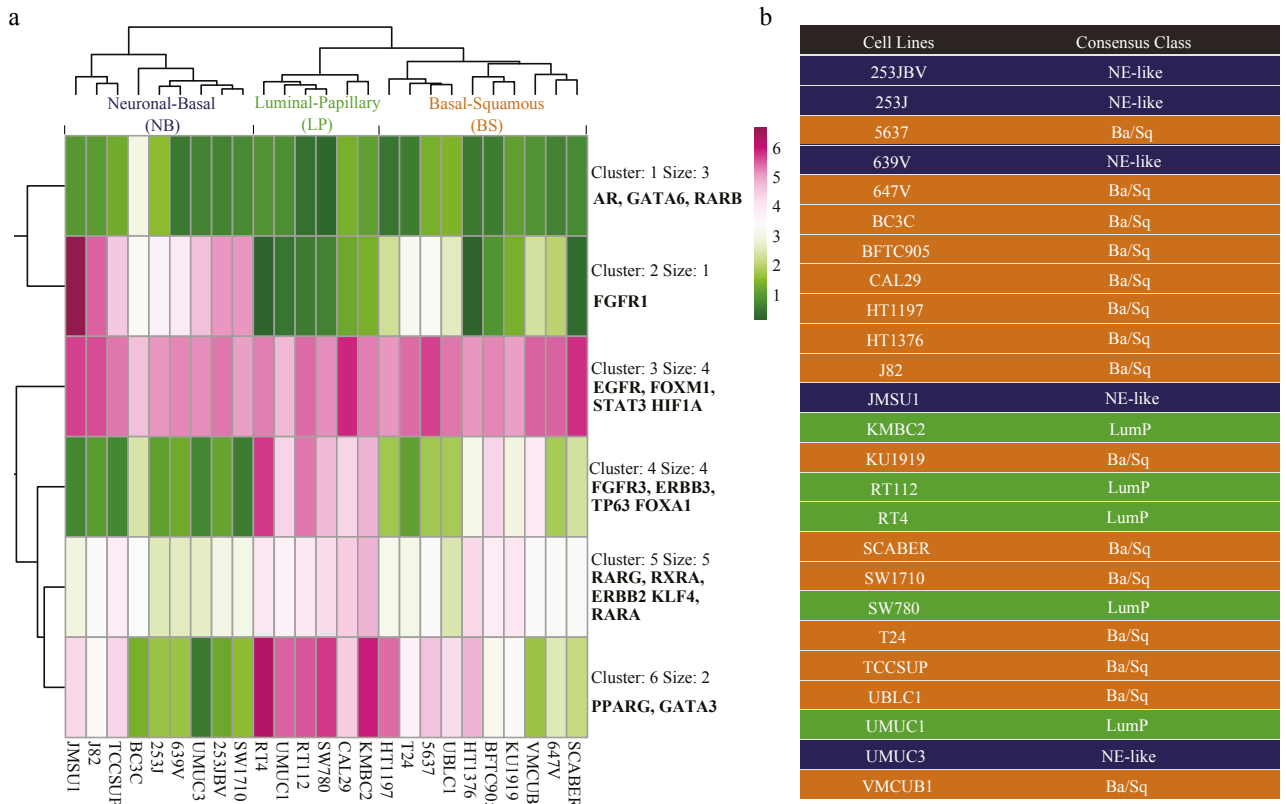
Figure 1. Clustering of bladder cancer cell lines according to regulon expressions (a) Heatmap visualization for the k-means clustering (k = 6) of regulon expressions in bladder cancer cell lines. Three cell line groups were represented as follows: the first group defined as Neuronal-Basal (NB), the second group defined as Luminal-Papillary (LP), the third group defined as Basal-Squamous (BS). (b) Consensus class assigned to bladder cancer cell lines. The table shows the consensus classes of the cell lines (output from the classifier for muscle invasive bladder cancer (Kamoun, et al. 2020).

determined as 5 if the number of the genes in upregulated gene set was >100, otherwise the number was set as 4 genes minimum. Genes, which are linked with at least 4 different GO terms, were displayed on the plots together with their logFC value representations.

2.3.5. Association of differentially expressed genes with the target genes of regulons
Regulon – target gene association table was downloaded from (Robertson et al., 2017) (Table S2.25) (Robertson et al., 2017). Genes, which are positively associated with the regulons (having value=1), were referred to as the target of the respective regulons. Afterwards, upregulated genes for each cell line group were intersected with the targets of the regulons and the results were presented as percent intersection rate (Figure 2).

2.4. Statistical analysis
Statistical analyzes were performed utilizing the R/Bioconductor packages (www.bioconductor.org). ANOVA was used to check the statistical difference among the groups for Figures 3a, 4a, 5a, and Supplementary Figure

S2. Subsequently, Bonferroni post-hoc test was applied to the results of ANOVA test. Spearman correlation test was applied for Figures 3c, 3d, 4c, 4d, and 5b. Dunnett's multiple comparisons test was used for statistical analysis of the immunostaining images (Figure 6b).

3. Results

3.1. Grouping of bladder cancer cell lines according to regulon activity
We determined the expression of the regulon genes in 25 bladder cancer cell lines and classified these cell lines according to the expression profile of the regulon genes. Our unsupervised clustering analysis using kmeans (k = 6) clustered the bladder cell lines into 3 groups (Figure 1a). In order to find out to what extent our regulon-based classifications are legitimate, we additionally classified the cell lines using the consensus classifier algorithm provided in (Kamoun et al., 2020). This analysis identified 5 out of 9 cell lines in group 1 to be assigned to neuroendocrine-like subgroup; 6 out of 6 cell lines in group 2 were identified to

Figure 2. Concordance of upregulated genes in cell line groups with regulon targeting. Percentages of NB and LP upregulated genes intersecting with regulon target genes. Intersection rates are displayed from red to green (red: high, green: low).

belong to luminal papillary and 10 out of 10 cell lines in group 3 as basal-squamous (Figure 1b). Among the group 1 cell lines, one cell line (J82) had almost equal annotation scores (0.383 vs 0.385) for neuroendocrine-like and basal squamous classes, and, for two of the cell lines (SW1710 and TCCSUP), annotation scores were rather close as well (Supplementary Table S1). Therefore, we named the group 1-3 as 'neuronal-basal (NB)', 'luminal papillary (LP)' and 'basal squamous (BS)', respectively.

Although luminal and basal terms are classically used for bladder cancer cell lines (Choi et al., 2014; Zuiverloon et al., 2018), our regulon expression-based analysis here brought additional features, characteristics of each group. Our analysis revealed that the expression status of *FGFR1*, which is highly enriched in 'stromal-rich' subgroup in consensus classification of bladder cancer (Kamoun et al., 2020), mainly separates the NB group from the two other groups. The regulon cluster 4 driven by the expression of *FGFR3*, *ERBB3*, *TP63,* and *FOXA1* was mainly enriched for LP class; regulon cluster 6 constituted by *PPARG* and *GATA3* expression was enriched in LP class and partially

in BS class. Regulon cluster 5, driven by luminal-papillary markers *RARG, RXRA* (Kamoun et al., 2020) and basal marker *KLF4* (Kamoun et al., 2020) was relatively enriched in LP class, with partial enrichments in NB and BS classes. Regulon cluster 3, dominated by the basal markers, *EGFR, FOXM1*, *STAT3* ,and *HIF1A* (Kamoun et al., 2020) were similarly enriched in all cell line groups.

3.2. Differential gene expression in bladder cell line groups and association with regulon activity

For each of the 3 groups, we determined with the clustering analysis (Figure 1a), we performed differential gene expression analysis contrasting one group with all other groups and determined the upregulated genes for each group. This analysis identified 327 and 570 upregulated genes in NB and LP classes, respectively. However, within the significance thresholds we used, we failed to detect upregulated genes for the BS class. The reason behind this can be attributed to the heterogeneous structure of this group, as it can be seen in the heatmap (Figure 1a) and in PCA analysis (Supplementary Figure S1) as well.

Having determined the upregulated genes in different cell line groups we defined, next, we tempted to relate those genes with the regulon targets. We identified the genes positively associated with the regulons using the information provided in (Robertson et al., 2017). This analysis showed that cell line groups constituted according to regulon expression profiles were in concordance with the regulon activity. For the NB group, upregulated genes had the highest intersection rate with *FGFR1* targets (18.96%), followed by *GATA6* (4.89%) and *FOXM1* (4.89%) (Figure 2). *FGFR1* was also significantly upregulated in the NB group (Figure 3a). *FGFR1* targets, which are upregulated in the NB class were mainly involved in neurogenesis, neuron differentiation, nervous system development (Figure 3b). Further, expression of the genes *VIM* and *ZEB1* implicated in epithelial to mesenchymal transition (Takeyama et al., 2010; Pluciennik et al., 2015; Larsen et al., 2016; Wu et al., 2018), highly correlated with the expression of *FGFR1*, emphasizing the role of this regulon in the transcriptomic constitution of the NB group (Figure 3c-3d).

Upregulated genes in the LP class mainly intersected with *ERBB2, FOXA1, PPARG, ERBB3, FGFR3, RARG,* and *GATA3* targets (Figure 2). We identified that almost all these regulons were significantly upregulated in the LP class (Figure 4a, Supplementary Figure S2). Target genes of the regulons upregulated in LP class were involved in epithelial cell differentiation, cell junction organization, and urogenital system development (Figure 4b, Supplementary Figure S2). Remarkably, expressions of *FOXA1* ($\rho = 0.71$) and *GRHL3* ($\rho = 0.60$) significantly correlated with the expression of *ERBB2* (Figure 4c-4d), indicating the luminal characteristics of the LP group.
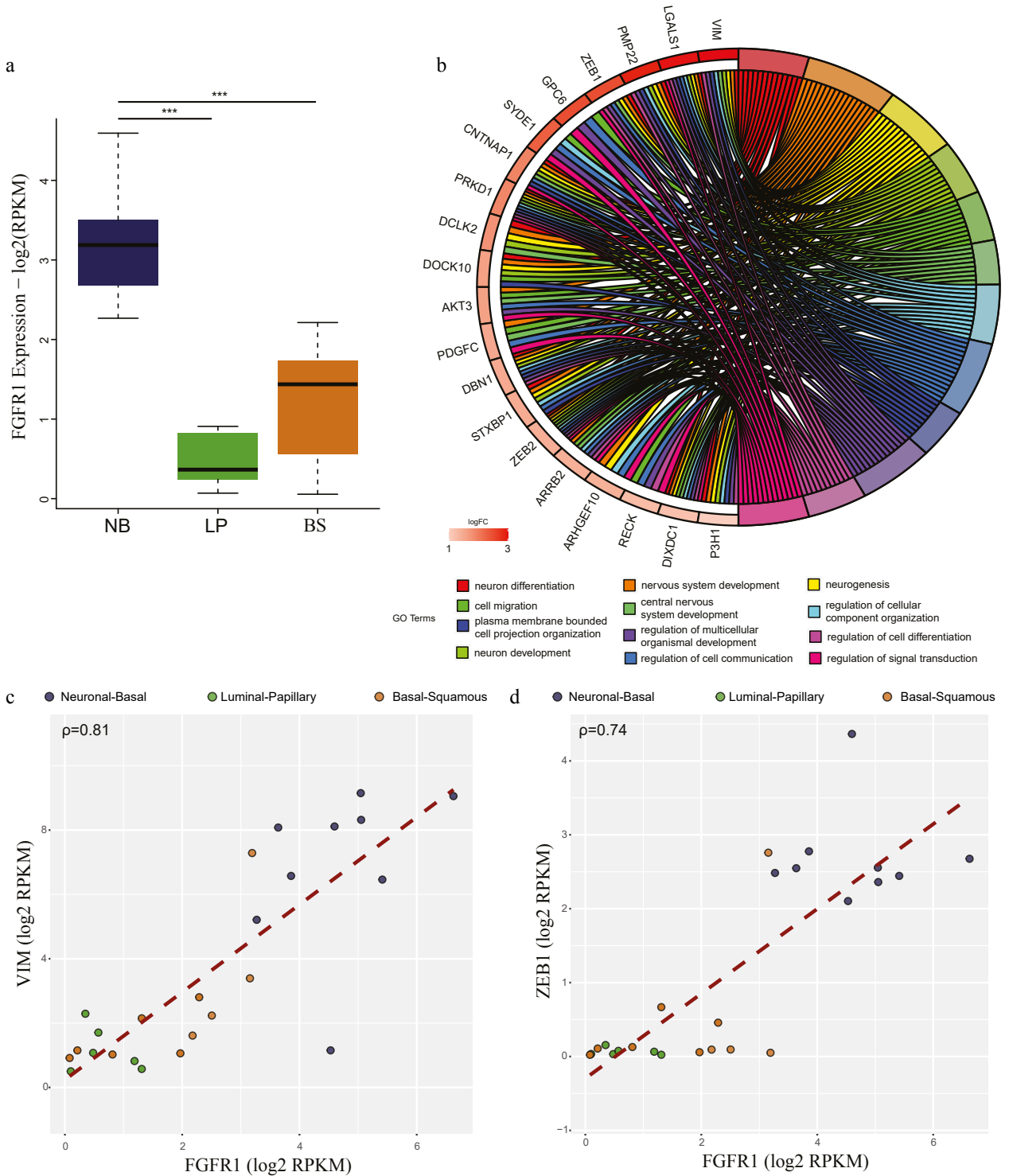
Figure 3. FGFR1 targets upregulated in NB group are involved in neuronal differentiation. (a) Boxplot comparing the expression of *FGFR1* in three cell line groups: Neuronal-Basal (NB) (dark blue), Luminal-Papillary (LP) (green) and Basal-Squamous (BS) (orange) (ANOVA p-value=1.24e-07). Bonferroni post-hoc test was used for statistical analysis (*p < 0.05; **p < 0.01; ***p < 0.001). (b) Chord plot visualization of GO term analysis applied to the genes upregulated in NB group cell lines and intersecting with *FGFR1* regulon targets. The right part of the chord plot represents the go terms, and the left part represents the genes linked with the respective terms. Genes are colored according to their logFC values. (c-d) Scatter plots comparing the expression *FGFR1* with its target genes *VIM* (ρ = 0.81) (c) and *ZEB1* (ρ = 0.74) (d). Colors represent the cell line groups.
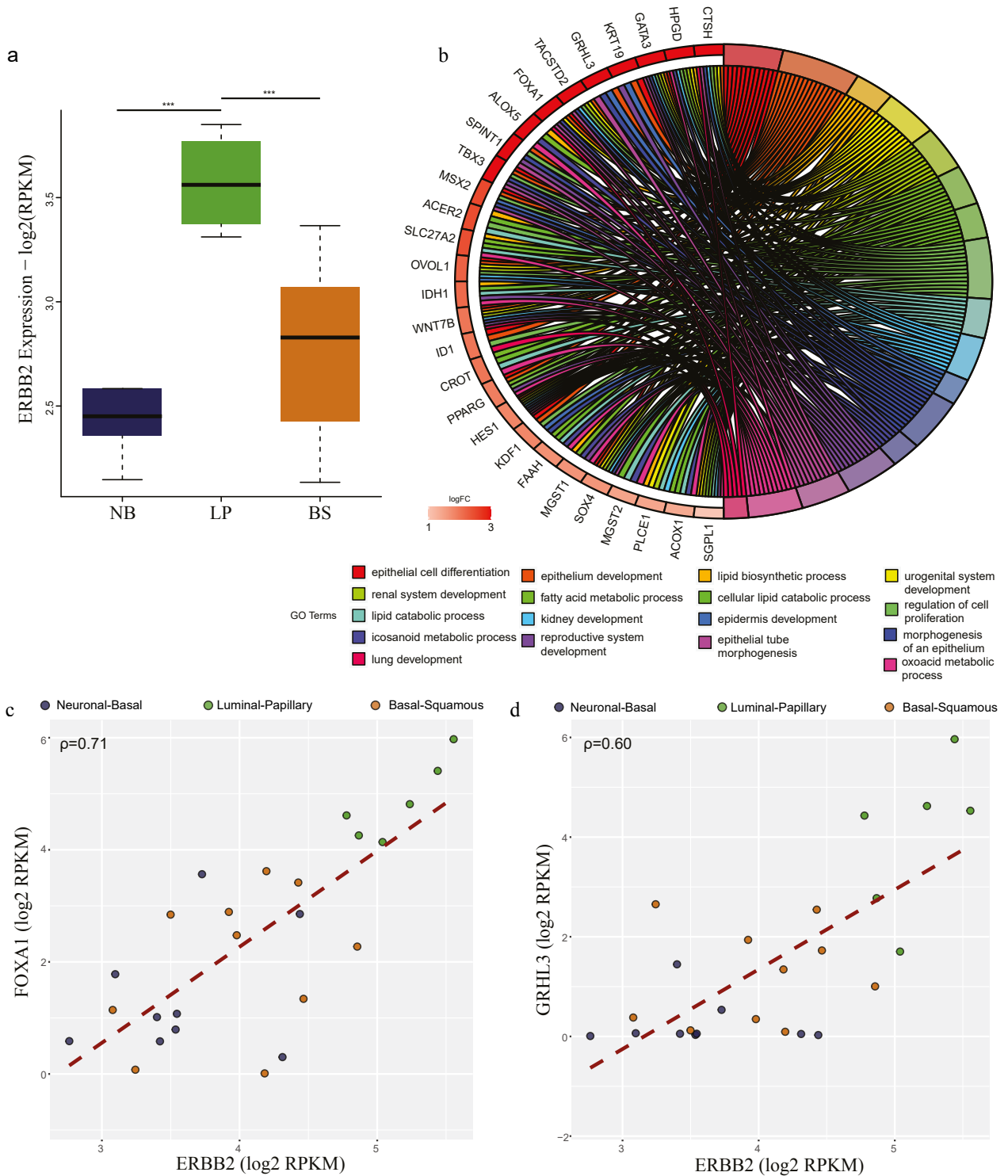
Figure 4. Targets of ERBB2 upregulated in LP group are implicated in epithelial morphogenesis. (a) Boxplot comparing the expression of *ERBB2* in three cell line groups: Neuronal-Basal (NB) (dark blue), Luminal-Papillary (LP) (green), and Basal-Squamous (BS) (orange) (ANOVA p-value=2.36e-05). Bonferroni post-hoc test was used for statistical analysis (*p < 0.05; **p < 0.01; ***p < 0.001). (b) Chord plot visualization of GO term analysis applied to the genes upregulated in LP group cell lines and intersecting with *ERBB2* regulon target genes. The right part of the chord plot represents the go terms, and the left part represents the genes associated with the terms. Coloring of the genes is done according to their expression of logFC values. (c-d) Scatter plot showing the correlation between the expression of *ERBB2* and its targets *FOXA1* (c) (ρ = 0.71) and *GRHL3* (ρ = 0.60) (d).

3.3. Cell lines belonging to NB-group expresses neuroendocrine differentiation marker genes

Our finding, which shows the enrichment of neurogenesis-related genes in the *FGFR1* targets upregulated in the NB group, prompted us to decipher this connection in more detail. As *FGFR1* is the main player characterizing this group, we checked the enrichment of *FGFR1* regulon activity in each consensus subgroup of primary bladder cancer (Kamoun et al., 2020). We discovered that although *FGFR1* has the highest enrichment score in stromal-rich consensus subgroup (Fisher's test p-value=4.20E-41), it was also moderately enriched in neuroendocrine-like subgroup (Fisher's test p-value= 3.18E-04) (Based on the information from Supplementary Table 3, (Kamoun et al., 2020)). To strengthen this association further, we checked the expression of genes marker of neuroendocrine differentiation (Kamoun et al., 2020) in the cell line groups we determined. This analysis also revealed that genes involved in neuroendocrine differentiation were significantly higher expressed in NB group (p-value=0.0146) (Figure 5a). Additionally, expression of *FGFR1* highly correlated with the expression of neuroendocrine markers (Figure 5b). Collectively, these results highly argue for the neuronal characteristics of the NE group and involvement of *FGFR1* in this signature.

3.4. J82 cells belonging to NB group show nucleocytoplasmic staining of β-catenin

We recently showed that the WNT/β-catenin pathway is associated with the active regulatory elements characterizing neuronal bladder cancer (Eray et al., 2020). Within this frame, to check any connection of the NB group with WNT/β-catenin pathway deregulation, we scanned the cell lines we used in this study for the mutation status of β-catenin and β-catenin destruction complex components. Among the NB group cell lines, 3 of them had *APC* mutation and one had *CTNNB1* mutation. On the contrary 2 had *APC* or *CTNNB1* mutation in the two other cell line groups (Supplementary Figure S3). Based on this information, we checked the β-catenin localization in one of the NB group cell lines we had in lab J82 and the other two cell lines, 5637 (BS group) and RT112 (LP group) as controls (no mutation in *CTNNB1* or *APC*). The staining of β-catenin in 5637 and RT112 was concentrated at the cytoplasm and the membrane while in J82 it was concentrated at the nucleus of the cells. Our data showed that β-catenin showed significantly higher nuclear localization in J82 compared to the other two cell lines (Figure 6a-6b). This finding strengthens our conclusions about the involvement of WNT/β-catenin pathway in neuronal differentiation of bladder cancer cells. The information we provide for the potential involvement of FGFR1 in neuroendocrine features of bladder cancer (Figure 5), identification of significantly increased nuclear localization of β-catenin in a cell line belonging to NB group (Figure 6) collectively strengthens the neuronal/neuroendocrine characteristics of the cell lines present in NB group according to our classifications.

4. Discussion

Bladder cancer cell lines serve as important models for modeling bladder tumorigenesis, invasive characteristics and treatment responses (Brown et al., 1990; Makridakis et al., 2009). So far, several studies characterized the genomic and transcriptomic properties of bladder cancer cell lines (Earl et al., 2015; Nickerson et al., 2017). In this study, we aimed to characterize the bladder cancer lines in terms of their regulon activity, defined for the primary bladder cancers in literature (Robertson et al., 2017; Lindskrog et al., 2021). Our results showed that bladder cancer cell lines have differential regulon activities, reflecting their transcriptomic signatures and their consensus classifications (Kamoun et al., 2020).

Genes significantly upregulated in cell lines belonging to the NB group were mainly intersected the targets of *FGFR1* and were involved in neuronal differentiation. Accordingly, the expression of the genes marker of neuroendocrine differentiation (Kamoun et al., 2020) was significantly higher in the NB group compared to the two other cell line groups. In literature, *FGFR1* has been shown be expressed at higher levels in bladder cancers showing mesenchymal features (Cheng et al., 2013). Knock-down of *FGFR1* in JMSU1 and UMUC3 cell lines, belonging to NB group in our results, resulted in a significant reduction in the anchorage-independent ability of these cells (Tomlinson et al., 2009). Further *FGFR1* expression was high in most small cell carcinoma of the bladder (Yang et al., 2020), which is a rare type of bladder cancer with neuroendocrine differentiation (Ghervan et al., 2017; Wang et al., 2019). These existing literature and our findings highly support the association of *FGFR1* with NB characteristics and neuronal differentiation of bladder cancer.

We previously showed that WNT/β-catenin pathway is deregulated in neuronal subtype of bladder cancer (Eray et al., 2020). In this study, we identified significantly higher accumulation β-catenin in nucleus in J82 cell line belonging to NB group, which has a mutation in *APC*, a component of β-catenin destruction complex (Krishnamurthy and Kurzrock 2018; Parker and Neufeld 2020). It is known that the immune gene expression signature is relatively depleted from small cell neuroendocrine carcinoma of the bladder (Yang et al., 2020), and neuroendocrine-like bladder cancer show decreased levels of immune infiltrate (Kamoun et al., 2020). It was also identified that Wnt/β-catenin signaling can decrease the T-cell infiltration in melanoma mouse models. Thus, inhibition of Wnt signaling has been suggested to prevent immunotherapy resistance (Chehrazi-Raffle et al., 2021). In addition,
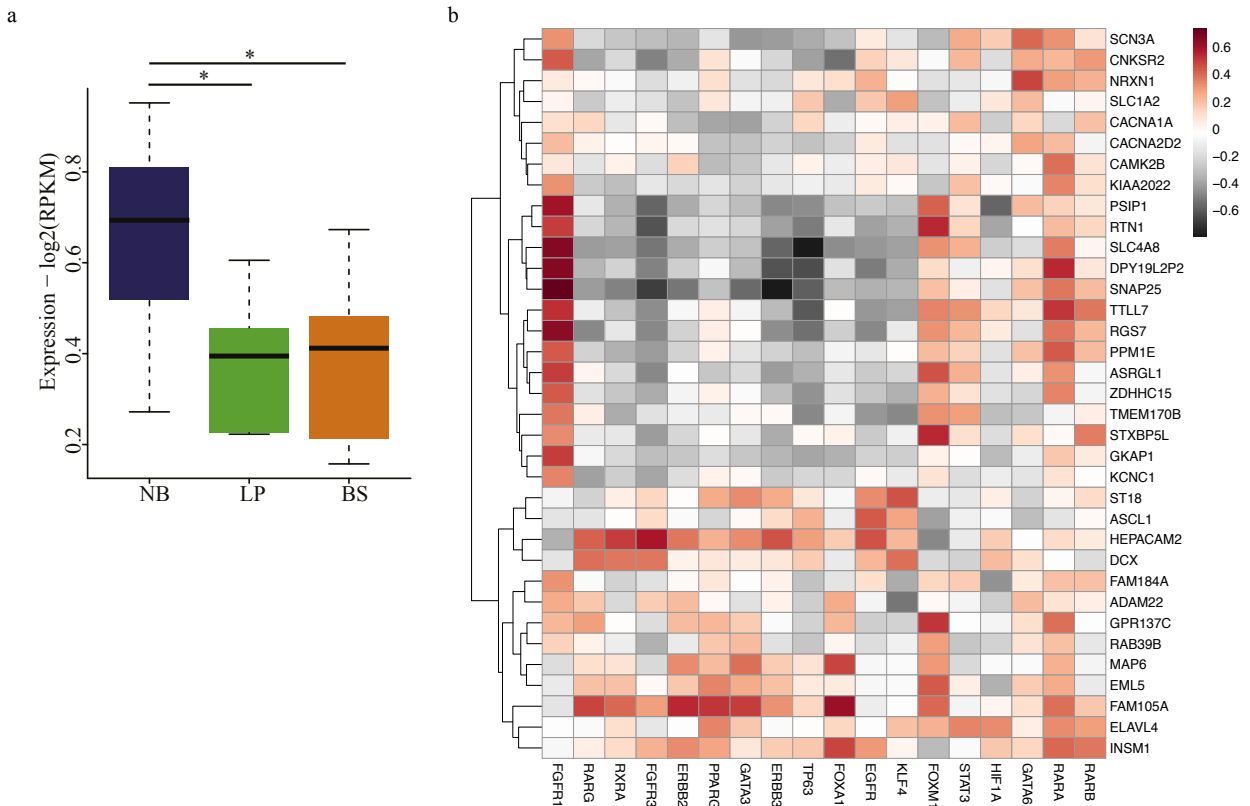
Figure 5. Expression profile of neuroendocrine marker genes in NB group (a) Boxplot shows the expression profile of genes associated with neuroendocrine differentiation (Kamoun, et al. 2020) in three cell line groups: Neuronal-Basal (NB) (dark blue), Luminal-Papillary (LP) (green) and Basal-Squamous (BS) (orange). (ANOVA p-value=0.0146). Bonferroni post-hoc test was used for statistical analysis (*p < 0.05; **p < 0.01; ***p < 0.001). (b) Heatmap displaying the correlation between the expression of genes involved in neuroendocrine differentiation and expression of regulons.

inhibition of *FGFR1* has been shown to enhance the immune checkpoint inhibitor response in breast cancer (Akhand et al., 2020). Based on all these information, we checked the expression of *CXCL16*, T cell chemoattractant (Akhand et al., 2020) in bladder cancer cell lines and identified a significant negative correlation with *FGFR1* expression (Supplementary Figure S4). Our data and existing literature together suggest a regulatory axis involving *FGFR1*, WNT/ β-catenin signaling, and tumor immune microenvironment in regulation of NB cell lines. Therefore, we suggest that combinatorial treatment strategies disrupting this regulatory axis can be applied on NB cell lines.

Regulons implicated in LP group cell lines are mainly known for early bladder cancer, mostly non-muscle invasive and luminal associations. *ERBB2* has been identified to be overexpressed in high-risk non-muscle invasive bladder cancer (Hedegaard et al., 2016) and as one of the major prognostic factors for survival status of the patients (Cormio et al., 2017; Moustakas et al., 2020). *FOXA1* expression was adequate for separating non-basal

subtype of bladder cancer from the basal subtype (Sikic et al., 2020). Furthermore, *GATA3*, *FOXA1*, and *PPARG* have been shown to drive the luminal fate in a collaborative manner (Warrick et al., 2016). Thus, within this frame, our regulon-based classifications confirm the luminal character of the LP class we defined.

Our differential gene expression analysis did not identify significantly upregulated genes in the BS class, largely because of the heterogeneity of this group (Supplementary Figure S1). However, we determined *EGFR, FOXM1 and STAT3* as the main regulons, driving the basal characterization of this group (cluster 3, Figure 1a). *EGFR* has been previously shown to be enriched in basal-like bladder cancer, and some groups of muscle invasive bladder cancers have been determined to respond to *EGFR* inhibitors (Rebouissou et al., 2014). In addition, expression of *FOXM1* as a prognostic factor in the survival of muscle invasive bladder cancer patients (Rinaldetti et al., 2017), *STAT3* expression, and phosphorylation was identified to be substantially higher in basal-like bladder cancer (Gatta et al., 2019). Further, *STAT3* activated
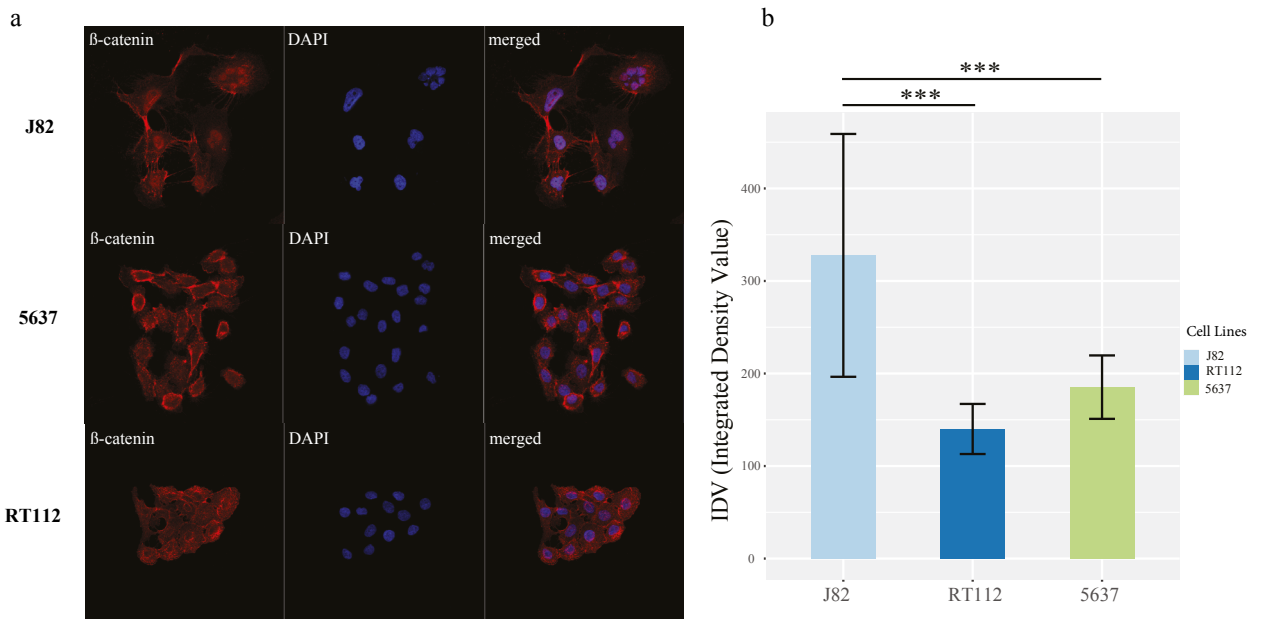
Figure 6. Immunostaining profile of β-catenin in cell line groups (a) Immunofluorescence images showing the staining of β-catenin cells; J82, 5638, and RT112. DAPI (blue) and β-catenin (red). (b) Barplot shows the quantification of nuclear signal in IF stainings. Dunnett's multiple comparisons test was used for statistical analysis (*p < 0.05; **p < 0.01; ***p < 0.001).

transgenic mice directly developed invasive bladder cancer without going through the intermediate noninvasive stages (Ho et al., 2012). Our results here collectively emphasize the role of *EGFR*, *FOXM1*, and *STAT3* in basal characteristics of BS cell lines.

To conclude, our regulon-based classification of bladder cancer cell lines may serve as an important guideline for studying the different regulons implicated in bladder cancer and trial of drug candidates relevant for targeting regulons.

Authorship contribution statement
Aleyna Eray: Design of the study, computational and experimental analysis, writing of the manuscript.

Serap Erkek-Ozhan: Design, supervision of the study, writing of the manuscript.

Declaration of Competing Interest
Authors declare no competing interests.

References

Akhand SS, Liu Z, Purdy SC, Abdullah A, Lin H et al. (2020). Pharmacologic Inhibition of FGFR Modulates the Metastatic Immune Microenvironment and Promotes Response to Immune Checkpoint Blockade. Cancer Immunol Research 8: 1542-1553.

Barretina J, Caponigro G, Stransky N, Venkatesan K, Margolin AA et al. (2012). The Cancer Cell Line Encyclopedia enables predictive modelling of anticancer drug sensitivity. Nature 483: 603-607.

Brown JL, Russell PJ, Philips J, Wotherspoon J, Raghavan D (1990). Clonal analysis of a bladder cancer cell line: an experimental model of tumour heterogeneity. British Journal of Cancer 61: 369-376.

Cancer Genome Atlas Research N (2014). Comprehensive molecular characterization of urothelial bladder carcinoma. Nature 507: 315-322.

Cerami E, Gao J, Dogrusoz U, Gross BE, Sumer SO et al. (2012). The cBio cancer genomics portal: an open platform for exploring multidimensional cancer genomics data. Cancer Discovery 2: 401-404.

Chehrazi-Raffle A, Dorff TB, Pal SK, Lyou Y (2021). Wnt/beta-Catenin Signaling and Immunotherapy Resistance: Lessons for the Treatment of Urothelial Carcinoma. Cancers 13: (4): 889. doi: 10.3390/cancers13040889

Cheng T, Roth B, Choi W, Black PC, Dinney C et al. (2013). Fibroblast growth factor receptors-1 and -3 play distinct roles in the regulation of bladder cancer growth and metastasis: implications for therapeutic targeting. PloS One 8: e57284.

Choi W, Porten S, Kim S, Willis D, Plimack ER et al. (2014). Identification of distinct basal and luminal subtypes of muscle-invasive bladder cancer with different sensitivities to frontline chemotherapy. Cancer Cell 25: 152-165.

Cormio L, Sanguedolce F, Cormio A, Massenio P, Pedicillo MC et al. (2017). Human epidermal growth factor receptor 2 expression is more important than Bacillus Calmette Guerin treatment in predicting the outcome of T1G3 bladder cancer. Oncotarget 8: 25433-25441.

Earl J, Rico D, Carrillo-de-Santa-Pau E, Rodriguez-Santiago B, Mendez-Pertuz M et al. (2015). The UBC-40 Urothelial Bladder Cancer cell line index: a genomic resource for functional studies. BMC Genomics 16: 403.

Eray A, Guneri PY, Yilmaz GO, Karakulah G, Erkek-Ozhan S (2020). Analysis of open chromatin regions in bladder cancer links beta-catenin mutations and Wnt signaling with neuronal subtype of bladder cancer. Scientific Reports 10: 18667.

Gao J, Aksoy BA, Dogrusoz U, Dresdner G, Gross B et al. (2013). Integrative analysis of complex cancer genomics and clinical profiles using the cBioPortal. Science Signaling 6 (269): pl1. doi: 10.1126/scisignal.2004088

Gatta LB, Melocchi L, Bugatti M, Missale F, Lonardi S et al. (2019). Hyper-Activation of STAT3 Sustains Progression of Non-Papillary Basal-Type Bladder Cancer via FOSL1 Regulome. Cancers 11 (9): 1-25. doi: 10.3390/cancers11091219

Ghervan L, Zaharie A, Ene B, Elec FI (2017). Small-cell carcinoma of the urinary bladder: where do we stand? Clujul Medical 90: 13-17.

Hedegaard J, Lamy P, Nordentoft I, Algaba F, Hoyer S et al. (2016). Comprehensive Transcriptional Analysis of Early-Stage Urothelial Carcinoma. Cancer Cell 30: 27-42.

Ho PL, Lay EJ, Jian W, Parra D, Chan KS (2012). Stat3 activation in urothelial stem cells leads to direct progression to invasive bladder cancer. Cancer Research 72: 3135-3142.

Jin X, Yun SJ, Jeong P, Kim IY, Kim WJ et al. (2014). Diagnosis of bladder cancer and prediction of survival by urinary metabolomics. Oncotarget 5: 1635-1645.

Kamburov A, Pentchev K, Galicka H, Wierling C, Lehrach H et al. (2011). ConsensusPathDB: toward a more complete picture of cell biology. Nucleic Acids Research 39: D712-717.

Kamburov A, Wierling C, Lehrach H, Herwig R (2009). ConsensusPathDB--a database for integrating human functional interaction networks. Nucleic Acids Research 37: D623-628.

Kamoun A, de Reynies A, Allory Y, Sjodahl G, Robertson AG et al. (2020). A Consensus Molecular Classification of Muscle-invasive Bladder Cancer. European Urology 77: 420-433.

Kolde R (2019). pheatmap: Pretty Heatmaps.

Krishnamurthy N, Kurzrock R (2018). Targeting the Wnt/beta-catenin pathway in cancer: Update on effectors and inhibitors. Cancer Treatment Reviews 62: 50-60.

Larsen JE, Nathan V, Osborne JK, Farrow RK, Deb D et al. (2016). ZEB1 drives epithelial-to-mesenchymal transition in lung cancer. Journal of Clinical Investigation 126: 3219-3235.

Lindskrog SV, Prip F, Lamy P, Taber A, Groeneveld CS et al. (2021). An integrated multi-omics analysis identifies prognostic molecular subtypes of non-muscle-invasive bladder cancer. Nature Communications 12: 2301.

Makridakis M, Gagos S, Petrolekas A, Roubelakis MG, Bitsika V et al. (2009). Chromosomal and proteome analysis of a new T24-based cell line model for aggressive bladder cancer. Proteomics 9: 287-298.

Moustakas G, Kampantais S, Nikolaidou A, Vakalopoulos I, Tzioufa V et al. (2020). HER-2 overexpression is a negative predictive factor for recurrence in patients with non-muscle-invasive bladder cancer on intravesical therapy. Journal of International Medical Research 48 (1): 300060519895847.

Nickerson ML, Witte N, Im KM, Turan S, Owens C et al. (2017). Molecular analysis of urothelial cancer cell lines for modeling tumor biology and drug response. Oncogene 36: 35-46.

Parker TW, Neufeld KL (2020). APC controls Wnt-induced beta-catenin destruction complex recruitment in human colonocytes. Scientific Reports 10: 2957.

Piantino CB, Sousa-Canavez JM, Srougi V, Salvadori F, Kato R et al. (2010). Establishment and characterization of human bladder cancer cell lines BexBra1, BexBra2, and BexBra4. In Vitro Cellular and Developmental Biology. Animal 46: 131-139.

Pinto-Leite R, Carreira I, Melo J, Ferreira SI, Ribeiro I et al. (2014). Genomic characterization of three urinary bladder cancer cell lines: understanding genomic types of urinary bladder cancer. Tumour Biology 35: 4599-4617.

Pluciennik E, Nowakowska M, Pospiech K, Stepien A, Wolkowicz M et al. (2015). The role of WWOX tumor suppressor gene in the regulation of EMT process via regulation of CDH1-ZEB1-VIM expression in endometrial cancer. International Journal of Oncology 46: 2639-2648.

Rebouissou S, Bernard-Pierrot I, de Reynies A, Lepage ML, Krucker C et al. (2014). EGFR as a potential therapeutic target for a subset of muscle-invasive bladder cancers presenting a basal-like phenotype. Science Translational Medicine 6: 244ra291.

Rinaldetti S, Wirtz RM, Worst TS, Eckstein M, Weiss CA et al. (2017). FOXM1 predicts overall and disease specific survival in muscle-invasive urothelial carcinoma and presents a differential expression between bladder cancer subtypes. Oncotarget 8: 47595-47606.

Robertson AG, Kim J, Al-Ahmadie H, Bellmunt J, Guo G et al. (2017). Comprehensive Molecular Characterization of Muscle-Invasive Bladder Cancer. Cell 171: 540-556 e525.

Sikic D, Eckstein M, Wirtz RM, Jarczyk J, Worst TS et al. (2020). FOXA1 Gene Expression for Defining Molecular Subtypes of Muscle-Invasive Bladder Cancer after Radical Cystectomy. Journal of Clinical Medicine 9 (4): 994. doi: 10.3390/jcm9040994

Sjodahl G, Lauss M, Lovgren K, Chebil G, Gudjonsson S et al. (2012). A molecular taxonomy for urothelial carcinoma. Clinical Cancer Research 18: 3377-3386.

Takeyama Y, Sato M, Horio M, Hase T, Yoshida K et al. (2010). Knockdown of ZEB1, a master epithelial-to-mesenchymal transition (EMT) gene, suppresses anchorage-independent cell growth of lung cancer cells. Cancer Letters 296: 216-224.

Tan TZ, Rouanne M, Tan KT, Huang RY, Thiery JP (2019). Molecular Subtypes of Urothelial Bladder Cancer: Results from a Meta-cohort Analysis of 2411 Tumors. European Urology 75: 423-432.

Tomlinson DC, Lamont FR, Shnyder SD, Knowles MA (2009). Fibroblast growth factor receptor 1 promotes proliferation and survival via activation of the mitogen-activated protein kinase pathway in bladder cancer. Cancer Research 69: 4613-4620.

Walter W, Sanchez-Cabo F, Ricote M (2015). GOplot: an R package for visually combining expression data with functional analysis. Bioinformatics 31: 2912-2914.

Wang Y, Li Q, Wang J, Tong M, Xing H et al. (2019). Small cell carcinoma of the bladder: the characteristics of molecular alterations, treatment, and follow-up. Medical Oncology 36: 98.

Warrick JI, Walter V, Yamashita H, Chung E, Shuman L et al. (2016). FOXA1, GATA3 and PPAR Cooperate to Drive Luminal Subtype in Bladder Cancer: A Molecular Analysis of Established Human Cell Lines. Scientific Reports 6: 38531.

Wu S, Du Y, Beckford J, Alachkar H (2018). Upregulation of the EMT marker vimentin is associated with poor clinical outcome in acute myeloid leukemia. Journal of Translational Medicine 16: 170.

Yang G, Bondaruk J, Cogdell D, Wang Z, Lee S et al. (2020). Urothelial-to-Neural Plasticity Drives Progression to Small Cell Bladder Cancer. iScience 23: 101201.

Zuiverloon TCM, de Jong FC, Costello JC, Theodorescu D (2018). Systematic Review: Characteristics and Preclinical Uses of Bladder Cancer Cell Lines. Bladder Cancer 4: 169-183.

Classification of bladder cancer cell lines according to regulon activity
**Supplementary Information**

Appendix A. Supplementary material
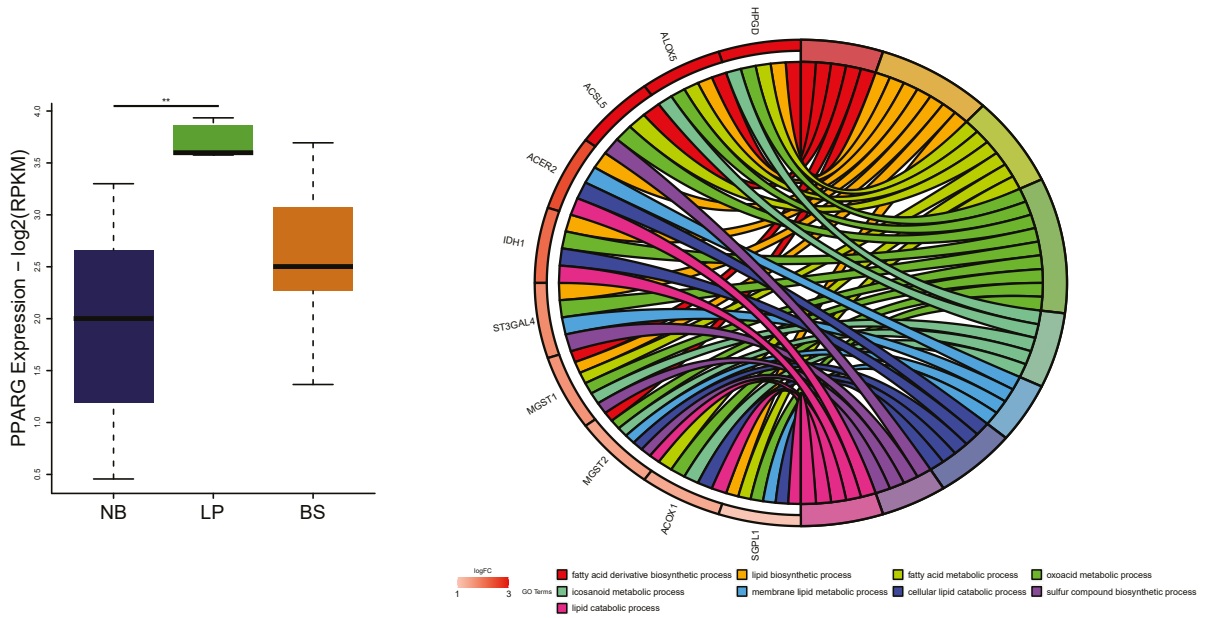**Supplementary data 1: Supplementary Figures 1–4.**
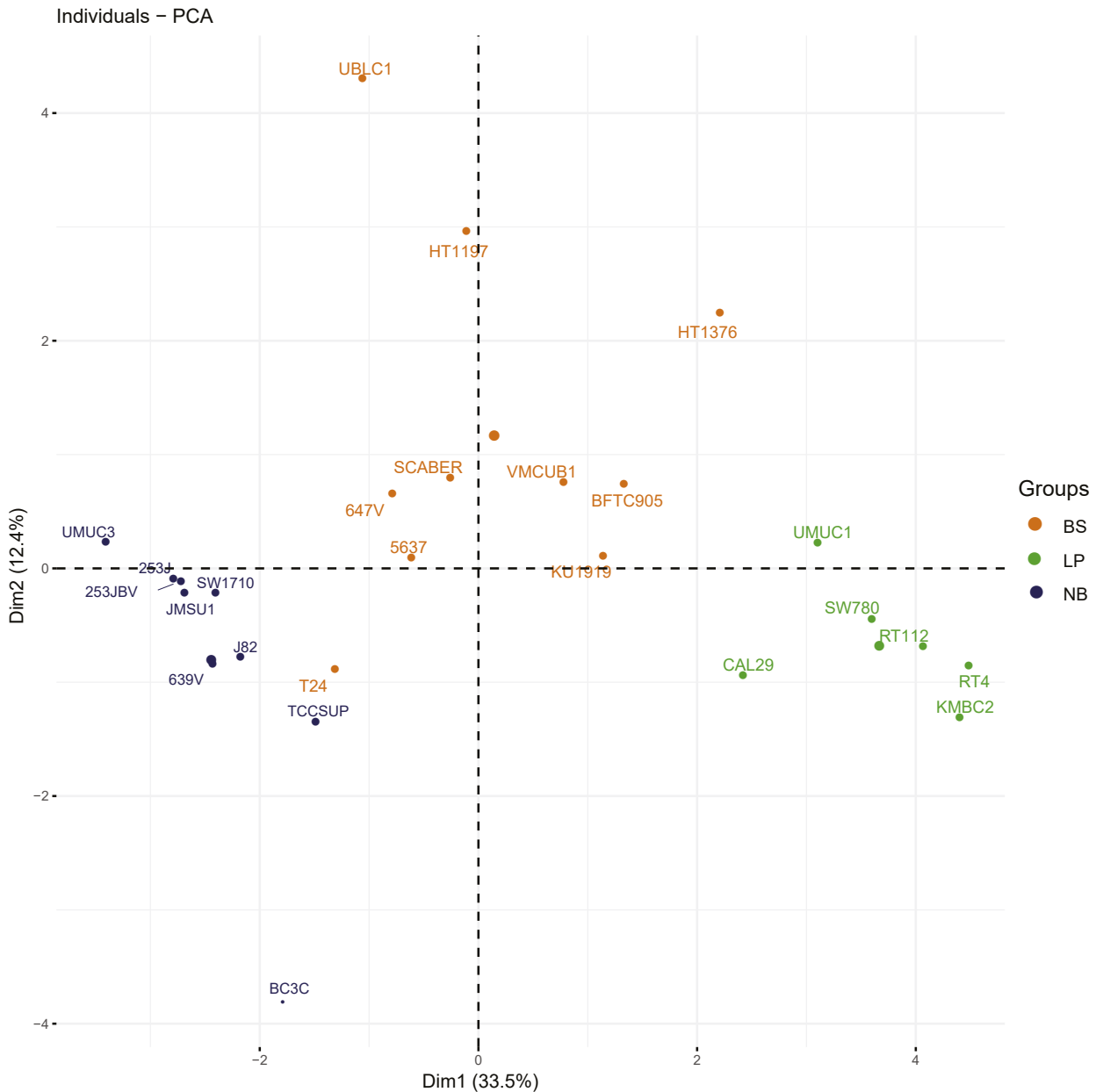
Supplementary Fig. S1. PCA plot of the bladder cancer cell lines according to their expression profiles. Group colors representing the determined bladder cancer cell line groups. Neuronal-Basal (NB) (dark blue), Luminal-Papillary (LP) (green) and Basal-Squamous (BS) (orange)
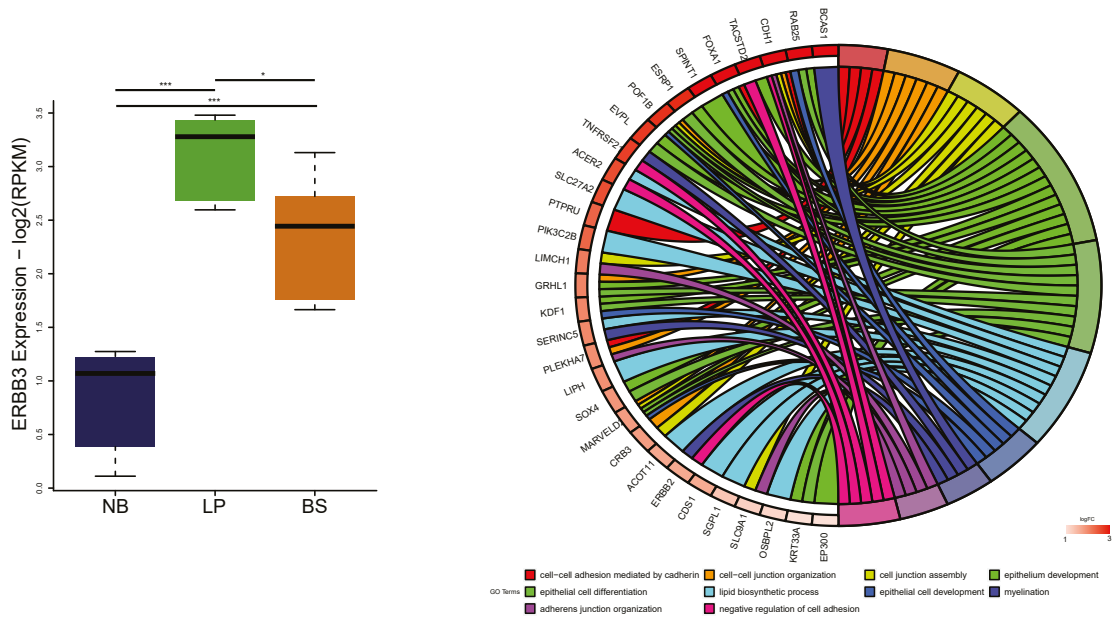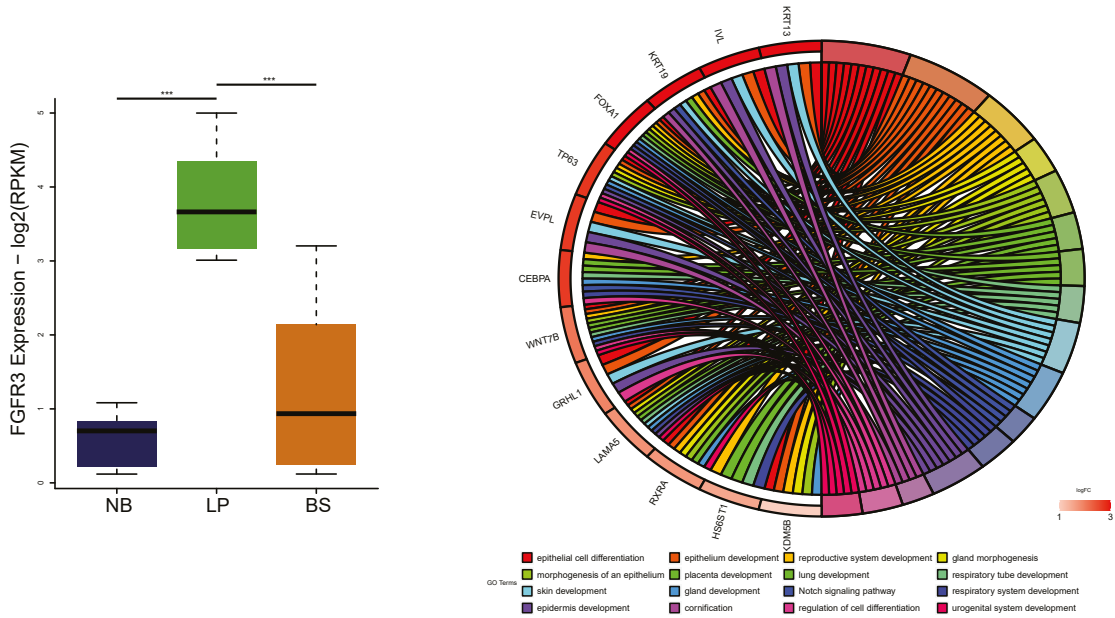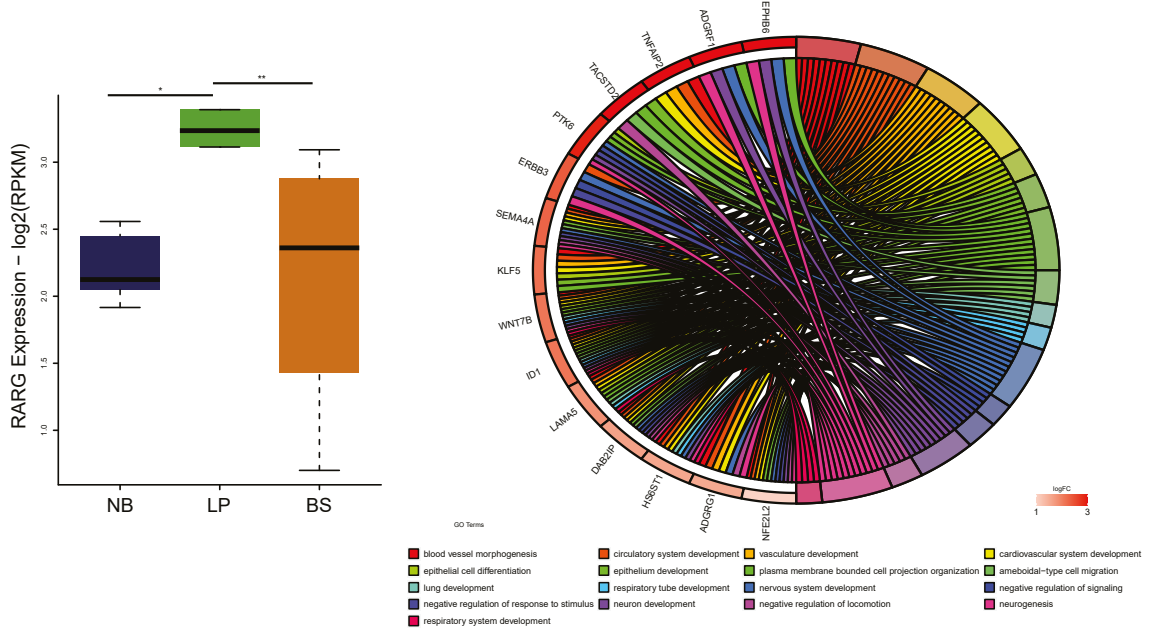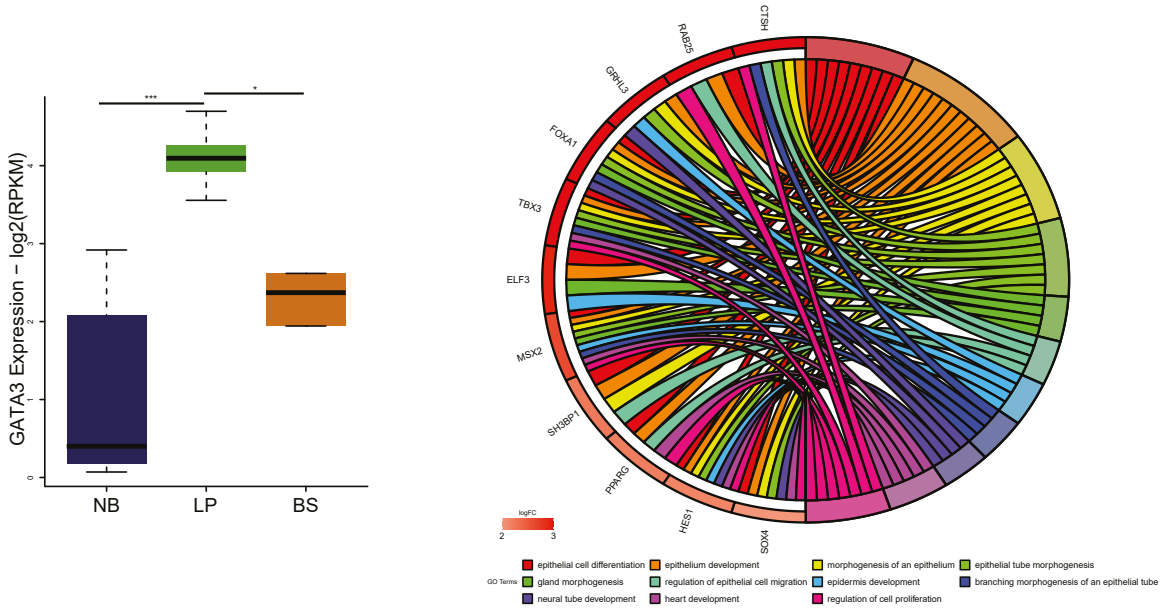
a

b

c

d
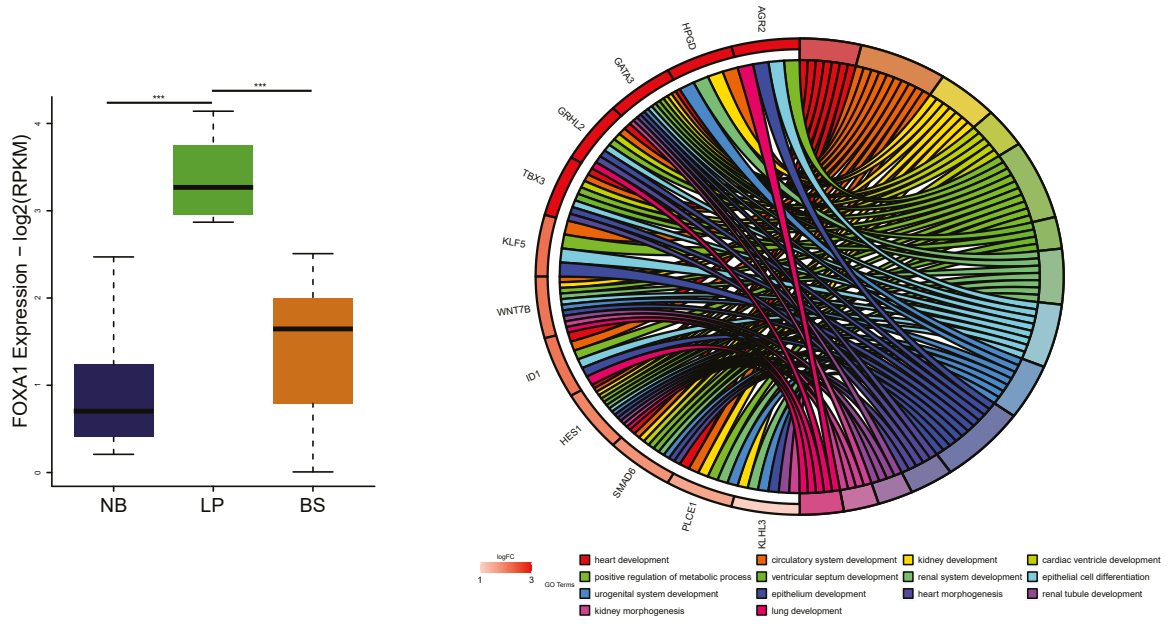
Supplementary Fig. S2. Targets of regulons upregulated in LP group are mostly associated with epithelial differentiation. Boxplots comparing the expression of FOXA1 (ANOVA p-value= 1.89e-05) (a), PPARG (ANOVA p-value=0.00498) (b), ERBB3 (ANOVA p-value=1.35e-06) (c), FGFR3 (ANOVA p-value=3.67e-07) (d), RARG (ANOVA p-value=0.00395) (e) and GATA3 (ANOVA p-value=0.000106) (f) in three cell line groups: Neuronal-Basal (NB) (dark blue), Luminal-Papillary (LP) (green) and Basal-Squamous (BS) (orange). Bonferroni post-hoc test was used for statistical analysis (*p<0.05; **p<0.01; ***p<0.001). Chord plot visualizations of GO term analysis applied to the genes upregulated in LP group cell lines and intersecting with the respective regulon target genes.
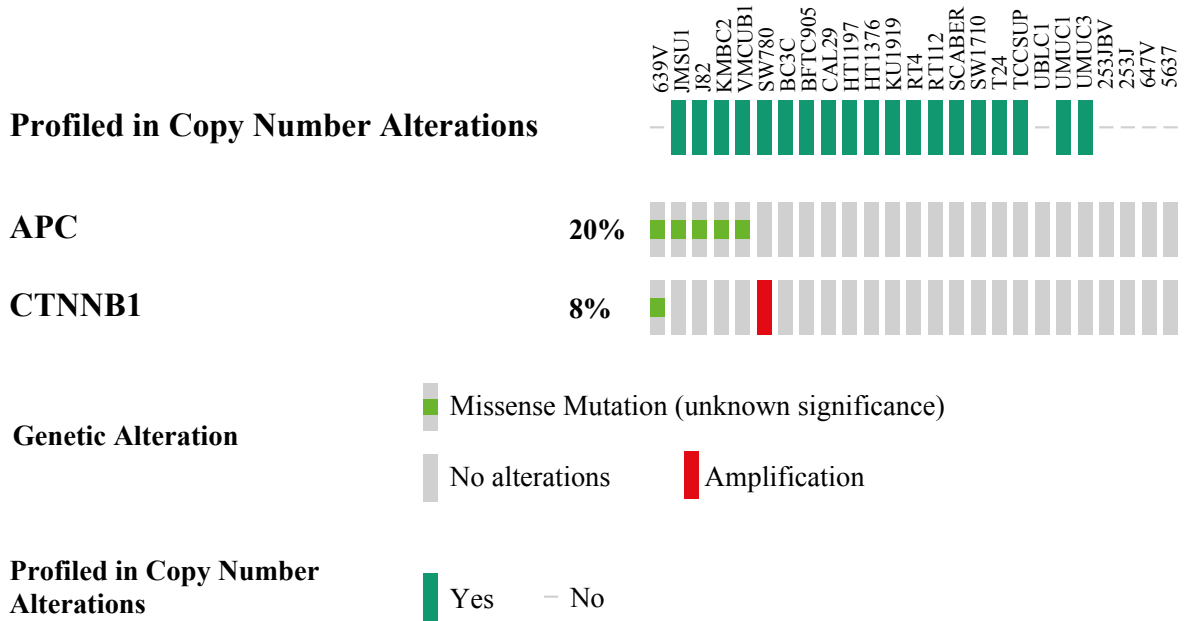
Supplementary Fig. S3. Oncoprint image of bladder cancer cell lines. APC and CTNNB1 (B-catenin) mutation and copy number alteration status of bladder cancer cell lines has shown.
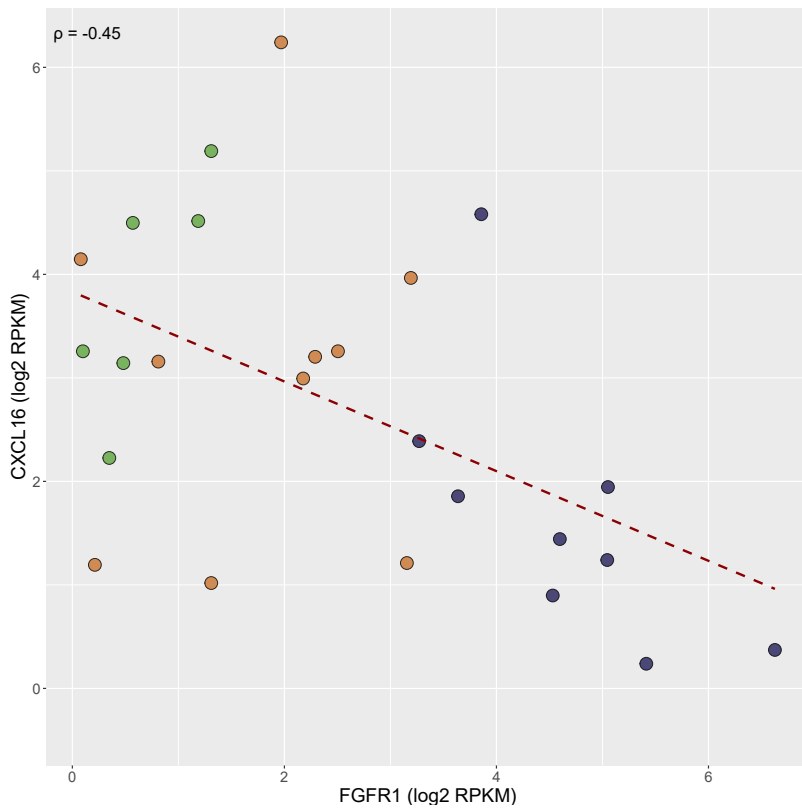
Supplementary Fig. S4. Correlation of FGFR1 and CXCL16 among bladder cancer cell lines. Scatter plot showing the correlation between the expression of FGFR1 and CXCL16 (ρ= -0.45).

Supplementary Table S1. Consensus classification table of bladder cancer cell lines.

Sample ID	consensusClass	cor_pval	separationLevel	LumP	LumNS	LumU	Stroma-rich	Ba/Sq	NE-like
253JBV_URINARY_TRACT	NE-like	4,68948E-24	0,093787156	0,2574151	0,189735587	0,247377733	0,198824769	0,329468504	0,337444966
253J_URINARY_TRACT	NE-like	8,42273E-21	0,053871132	0,255865753	0,193039385	0,244510671	0,196392919	0,309972265	0,313376277
5637_URINARY_TRACT	Ba/Sq	3,10386E-52	0,777526879	0,320335243	0,222932533	0,285254683	0,249088958	0,488967135	0,258914796
639V_URINARY_TRACT	NE-like	5,88916E-42	0,480284829	0,192728703	0,142214341	0,22542168	0,197533365	0,331390213	0,442205232
647V_URINARY_TRACT	Ba/Sq	1,54644E-47	0,853265862	0,360508926	0,299953032	0,363097861	0,315952481	0,468489991	0,32943872
BC3C_URINARY_TRACT	Ba/Sq	3,85491E-47	0,775646138	0,308196594	0,213172802	0,253708029	0,239951443	0,466695478	0,270994284
BFTC905_URINARY_TRACT	Ba/Sq	1,52316E-76	0,584423412	0,422818212	0,288666156	0,335488698	0,290741175	0,577093414	0,21967185
CAL29_URINARY_TRACT	Ba/Sq	3,30704E-59	0,220002263	0,492824834	0,387673587	0,426484928	0,350598546	0,517009803	0,247840408
HT1197_URINARY_TRACT	Ba/Sq	6,09385E-43	0,664541223	0,373748743	0,30814758	0,365380334	0,29417652	0,447015315	0,277811389
HT1376_URINARY_TRACT	Ba/Sq	4,64879E-57	0,592003049	0,418565222	0,331541917	0,381424854	0,303431822	0,508645886	0,236359508
J82_URINARY_TRACT	Ba/Sq	2,34935E-31	0,012885797	0,255052604	0,215409058	0,279418652	0,275533116	0,384827653	0,383444339
JMSU1_URINARY_TRACT	NE-like	1,00507E-30	0,435240446	0,192029012	0,134416904	0,211183064	0,181166748	0,302936915	0,381029081
KMBC2_URINARY_TRACT	LumP	3,86982E-71	0,721042702	0,559638686	0,43980401	0,477951587	0,344787233	0,452892887	0,162528213
KU1919_URINARY_TRACT	Ba/Sq	1,50534E-41	0,765579351	0,31610755	0,216494475	0,27204855	0,242037133	0,440192423	0,328330276
RT112_URINARY_TRACT	LumP	4,55157E-70	0,475389501	0,556054737	0,411844479	0,444996894	0,352912892	0,49537885	0,220265266
RT4_URINARY_TRACT	LumP	2,18981E-90	0,488905979	0,617489047	0,48873091	0,51529522	0,328196143	0,32483191	0,179469076
SCABER_URINARY_TRACT	Ba/Sq	1,23879E-63	0,778203729	0,28314435	0,1705654	0,210240712	0,213314677	0,5335444	0,159793097
SW1710_URINARY_TRACT	Ba/Sq	8,01706E-28	0,223664926	0,235561407	0,18319918	0,238596488	0,243605788	0,362888249	0,335648744
SW780_URINARY_TRACT	LumP	3,23431E-85	0,677347617	0,603068728	0,47822204	0,496243374	0,366094419	0,412492873	0,197484157
T24_URINARY_TRACT	Ba/Sq	1,04177E-35	0,281996728	0,288417557	0,206595387	0,2757358	0,257842078	0,409752767	0,373748528
TCCSUP_URINARY_TRACT	Ba/Sq	4,14267E-39	0,600646896	0,269844645	0,243464373	0,281987659	0,330848122	0,427852909	0,354913342
UBLC1_URINARY_TRACT	Ba/Sq	6,13272E-33	0,745331532	0,314657849	0,248066126	0,321962335	0,265617883	0,394141414	0,279941831
UMUC1_URINARY_TRACT	LumP	5,49414E-75	0,439865763	0,572170984	0,457405107	0,47096898	0,408079974	0,524672546	0,213547081
UMUC3_URINARY_TRACT	NE-like	1,6174E-28	0,416702796	0,157234364	0,089970968	0,170911571	0,135505835	0,282638522	0,367340793
VMCUB1_URINARY_TRACT	Ba/Sq	1,05499E-63	0,614207938	0,389584383	0,273083351	0,313249594	0,284754548	0,533797757	0,21824899